Available online at www.sciencedirect.com

ScienceDirect

Procedia Technology 23 (2016) 28 – 35

Procedia Technology

3rd International Conference on Innovations in Automation and Mechatronics Engineering, ICIAME 2016

Influence of Elliptic Bore and non-Newtonian Rheology of Lubricant on the Performance and Stability of Journal Bearing

F. Rahmani*, R. K. Pandey, and J. K. Dutt

Department of Mechanical Engineering, Indian Institute of Technology Delhi, New Delhi – 110016, India

Abstract

The objective of this paper is to present investigations related to the performance of fluid film journal bearings incorporating the synergistic effects of elliptic bore and non-Newtonian rheology of lubricant. The Rabinowitsch fluid model has been employed herein for simulating the non-Newtonian rheology of lubricant and Reynolds equation is developed accordingly. The performance parameters (load carrying capacity, coefficient of friction, and stability) of bearing have been investigated and discussed herein in terms of ellipticity (of bearing bore) and non-linearity parameter (relating the non-Newtonian rheology). The combined effects of shear thinning of the lubricant and increase in the ellipticity of the bearing bore cause reduction in the load carrying capacity and increase in friction coefficient in comparison to plain circular bore journal bearing lubricated with Newtonian lubricant. However, increase in the ellipticity of bore alone enhances the stability of the rotor-bearing system.

Peer-review under responsibility of the organizing committee of ICIAME 2016

Keywords: Bearing bore defects; Rabinowitsch fluid model; Dynamic coefficients; Rotor stability.

Nomenclature

c_{ij}	Damping coefficient, N-s/m
C_{ij}	Dimensionless damping coefficient, $C_{ij} = c_{ij}\left(C_r\omega/W\right)$
C_r	Radial clearance, m
e	Eccentricity, m

* Corresponding author. Tel.: +91 858 706 1099.
E-mail address: faisalrahmani@gmail.com

Peer-review under responsibility of the organizing committee of ICIAME 2016
doi:10.1016/j.protcy.2016.03.069

f	Coefficient of friction
$\bar{F}_{x,y}$	Dimensionless forces in X and Y directions, $\bar{F}_{x,y} = F_{x,y} C_r^2 / \eta_0 U R^2 L$
G	Ellipticity parameter, $G = (R_{max} - R_{min})/C_r$
$\bar{h}$	Dimensionless film thickness, $\bar{h} = h/C_r$
K_{ij}	Dimensionless stiffness coefficient, $K_{ij} = k_{ij}(C_r/W)$
L	Length of the bearing, m
m	mass, kg
$\bar{P}$	Dimensionless pressure, $\bar{P} = P C_r^2 / \eta_0 U R$
$\bar{P}_c$	Dimensionless cavitation pressure
R	Radius of journal, m
U	Journal surface velocity, m/s
$\bar{W}$	Dimensionless load, $\bar{W} = W C_r^2 / \eta_0 U R^2 L$
$\bar{x}$	Normalized x-coordinate, $\bar{x} = x/C_r$
$\Delta\bar{X}$	Normalized displacement perturbation in X-direction, $\Delta\bar{X} = \Delta X / C_r$
$\Delta\dot{\bar{X}}$	Normalized velocity perturbation in X-direction, $\Delta\dot{\bar{X}} = \Delta\dot{X} / (C_r\omega)$
$\bar{y}$	Normalized y-coordinate, $\bar{y} = y / C_r$
$\Delta\bar{Y}$	Normalized displacement perturbation in Y-direction, $\Delta\bar{Y} = \Delta Y / C_r$
$\Delta\dot{\bar{Y}}$	Normalized velocity perturbation in X-direction, $\Delta\dot{\bar{Y}} = \Delta\dot{Y} / (C_r\omega)$
$\bar{z}$	Normalized z-coordinate, $\bar{z} = z / L$

Greeks

α	Non-linearity parameter in Rabinowitsch fluid model
δ	Angle between the major axis of elliptic bore and load line, rad
ε	Eccentricity ratio (e/C_r)
$\bar{\eta}$	Dimensionless viscosity (η/η_0)
θ	Angle, rad
φ	Fraction of film content
ϕ	Attitude angle
ω	Journal angular speed, rad/s
$\bar{\tau}$	Dimensionless shear stress, $\bar{\tau} = \tau C_r^2 / (\eta_0 U)^2$

1. Introduction

Fluid film journal bearings are widely employed in rotating machinery for supporting the rotors for wide range of operating parameters. Usually it has been noticed that non-circularity defects in the bore of bearings develop at the micro-level during the operation due to the vibration, wear and misalignment at the interfaces of rotor/bearings. In the last couple of decades, many researchers [1-6] have attempted to address the performance parameters of the journal bearings having bore defects. The presence of surface imperfection [1] and non-circularity defects [2, 3] in bearing bore has substantially influenced the performance behaviours of journal bearings. Influence of ellipticity of bore on the performance of dynamically loaded journal bearing and dynamic behavior of the wavy rotor supported on journal bearings have been studied by Goenka and Booker [4] and Bonneau and Frêne [5], respectively. It has been reported that in the presence of wave form (defect) on the rotor, high magnitude of vibration commences even in the absence of unbalance forces [4]. In the stability studies of the rotors, the values of bearing coefficients (stiffness and damping) play vital role [7, 8]. Stability studies of rigid rotors supported on the fluid film journal

bearings have been presented by the authors [7-15] extracting the stiffness and damping coefficients of film through the linear perturbation approach. From practical aspects, the rotor stability studies incorporating the synergistic effects of bearing defects (ellipticity of the bore and orientation of its major axis with respect to the load line) and non-Newtonian rheology of the lubricant (due to additives mixed in the lubricant to improve its performance) have great significance. It is worth noting here that ellipticity in the bearing bore arises due to the operational issues (fluctuation/variation in operating parameters and circularity imperfections in the shafts) and manufacturing constraints. Thus, the objective of this paper is to present numerical study for exploring the influence of ellipticity of the bore (with its orientation) and non-Newtonian rheology (thinning) of the lubricant on the performance and stability of bearings.

2. Mathematical model

The non-circular bore bearing (having particular orientation with respect to the load line) with the coordinate system is shown in Fig. 1 along with representation of lubricating film by springs and dampers.

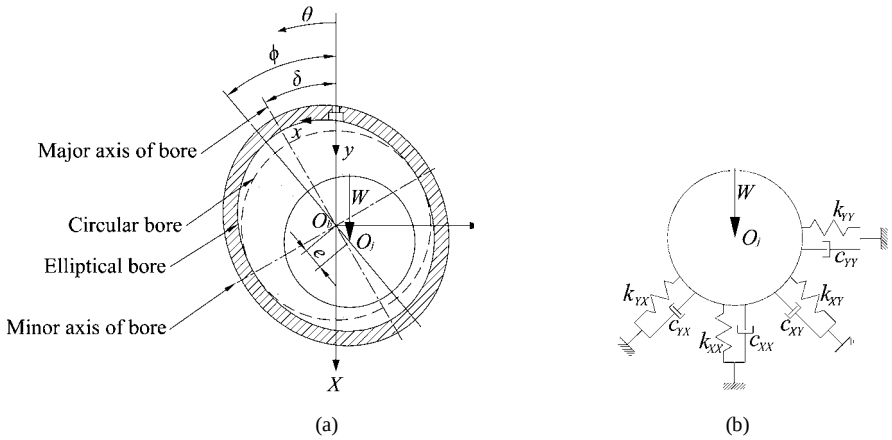

Fig. 1. (a) Schematic diagram of elliptic bore bearing with coordinate system, (b) Representation of film by springs and dampers

2.1. Film thickness relation

Normalized film thickness is expressed as [2]:

$$\bar{h} = 1 + G\cos^2(\theta - \delta) + \varepsilon\cos(\theta - \phi) = 1 + G\cos^2(\theta - \delta) + \bar{X}\cos\theta + \bar{Y}\sin\theta \tag{1}$$

where $\bar{X} = \varepsilon\cos\phi$, and $\bar{Y} = \varepsilon\sin\phi$. For elliptic bore, the radial clearance C_r is expressed as ($R_{min} - R$). Putting G = 0, eq. (1) reduces to the film thickness relation applicable for the circular bore.

2.2. Rheological relation

The performance parameters of the fluid film journal bearings operating for wide range of loads and speeds are normally improved by adding the polymeric additives of high molecular weight in the lubricating oil. Thus, the lubricating oil with additive behaves as a non-Newtonian fluid. Hence for representing the rheology of lubricating oil with the polymeric additive, the Rabinowitsch fluid model has been employed herein [16]. The Rabinowitsch fluid model given by eq. (2) has been used in the proposed investigation:

$$\bar{\tau}_{xy} + \alpha\bar{\tau}_{xy}^3 = \bar{\eta}\frac{\partial\bar{u}}{\partial\bar{y}} \tag{2}$$

where α is a factor accounting for the non-Newtonian effects ($\alpha > 0$ for pseudo-plastic, $\alpha < 0$ for dilatant, and $\alpha = 0$ for Newtonian fluids).

2.3. Modified Reynolds equation

The modified Reynolds equation [17] incorporating the non-Newtonian rheology (Rabinowitsch fluid model) and mass conservation algorithm [18-20] is written as:

$$\frac{\partial}{\partial\theta}\left[\bar{\eta}\left(\frac{\bar{h}^3}{12}+\alpha\frac{\bar{h}}{4}\right)\bar{\beta}g\frac{\partial\varphi}{\partial\theta}+\frac{\alpha}{\bar{\eta}}\frac{\bar{h}^5}{80}\left(\bar{\beta}g\frac{\partial\varphi}{\partial\theta}\right)^3\right]+\left(\frac{R}{L}\right)^2\frac{\partial}{\partial\bar{z}}\left[\frac{\bar{h}^3}{12\bar{\eta}}\bar{\beta}g\frac{\partial\varphi}{\partial\bar{z}}+\frac{\alpha}{\bar{\eta}}\frac{\bar{h}^5}{80}\left(\bar{\beta}g\frac{\partial\varphi}{\partial\bar{z}}\right)^3\right]$$
$$=\frac{1}{2}\left[\frac{\partial\left(\varphi\bar{h}\right)}{\partial\theta}+\bar{\eta}^2\alpha\frac{\partial}{\partial\theta}\left(\frac{1}{\varphi\bar{h}}\right)\right]+\frac{\partial\left(\varphi\bar{h}\right)}{\partial\bar{t}} \tag{3}$$

where, $\bar{\beta}=\beta C_r^2/\eta_0 UR$, $\bar{P}=\bar{P}_c+\bar{\beta}(\varphi-1)$. $\bar{P}_c$ is the cavitation pressure, and φ is the fraction of film content. g is a switch function which takes the value as $g = 0$ for $\varphi < 1$, and $g = 1$ for $\varphi \geq 1$.

2.4. Miscellaneous relations

Resultant load on the bearing is computed as:

$$\bar{W}=\sqrt{\bar{F}_X^2+\bar{F}_Y^2}=\sqrt{\left(\int_0^1\int_0^{2\pi}\bar{P}\cos\theta\,d\theta d\bar{z}\right)^2+\left(\int_0^1\int_0^{2\pi}\bar{P}\sin\theta\,d\theta d\bar{z}\right)^2} \tag{4}$$

Coefficient of friction is evaluated using the following relation:

$$f=\left(\frac{C_r}{R}\right)\left(\frac{1}{\bar{W}}\right)\int_0^1\int_0^{2\pi}\bar{\tau}_{xy_{\,at\,\bar{y}=\bar{h}}}\,d\theta d\bar{z} \tag{5}$$

2.5. Dynamic performance parameter

Stability of a rigid rotor (well-aligned rigid rotor of mass $2m$) supported on two identical elliptic bore journal bearings has been investigated in this paper. The direct and cross coupled stiffness and damping coefficients of the bearing have been computed using the finite perturbation approach [21]. The equations of motion for free vibration of the rotor- bearing system is written as:

$$\begin{bmatrix}m & 0\\ 0 & m\end{bmatrix}\begin{Bmatrix}\Delta\ddot{X}\\ \Delta\ddot{Y}\end{Bmatrix}+\begin{bmatrix}c_{XX} & c_{XY}\\ c_{YX} & c_{YY}\end{bmatrix}\begin{Bmatrix}\Delta\dot{X}\\ \Delta\dot{Y}\end{Bmatrix}+\begin{bmatrix}k_{XX} & k_{XY}\\ k_{YX} & k_{YY}\end{bmatrix}\begin{Bmatrix}\Delta X\\ \Delta Y\end{Bmatrix}=\begin{Bmatrix}0\\ 0\end{Bmatrix} \tag{6}$$

The solution of eq. (6) is taken as:

$$\begin{Bmatrix}\Delta X\\ \Delta Y\end{Bmatrix}=\begin{Bmatrix}X_h\\ Y_h\end{Bmatrix}e^{(\mu+i\nu)t} \tag{7}$$

For $\mu > 0$, the solution happens an exponentially growing function that will signify the instability. Hence for the system to be stable, μ must be negative. Therefore, the threshold of the stability is obtained keeping $\mu = 0$. Substituting eq. (7) in eq. (6) and putting $\mu = 0$, the following relationship is obtained:

$$\begin{bmatrix} (k_{XX} - m\nu^2 + i\nu c_{XX}) & (k_{XY} - i\nu c_{XY}) \\ (k_{YX} - i\nu c_{YX}) & (k_{YY} - m\nu^2 + i\nu c_{YY}) \end{bmatrix} \begin{Bmatrix} X_h \\ Y_h \end{Bmatrix} = \begin{Bmatrix} 0 \\ 0 \end{Bmatrix} \tag{8}$$

For the non-trivial solution, the determinant of the coefficient matrix in (refer eq. (8)) must be zero. Thus, equating the real and imaginary components of the determinant of the coefficient matrix to zero yields the following two equations (provided in the normalized form):

$$\lambda_{cr}^2 = \frac{(K_{XX} - K_{eq})(K_{XX} - K_{eq}) - K_{XY}K_{YX}}{C_{XX}C_{XX} - C_{XY}C_{YX}} \tag{9}$$

$$K_{eq} = \frac{C_{XX}K_{YY} + C_{YY}K_{XX} - C_{YX}K_{XY} - C_{XY}K_{YX}}{C_{XX} + C_{YY}} \tag{10}$$

where $\lambda_{cr} = \dfrac{\nu}{\omega}$ is whirl frequency ratio, $K_{eq} = m\nu^2 \dfrac{C_r}{W}$ is an equivalent stiffness. In the present study, the stability parameter is defined by critical mass $\left(M_{cr} = \dfrac{K_{eq}}{\lambda_{cr}^2} = m\omega^2 \dfrac{C_r}{W} \right)$.

3. Computational procedure

The modified Reynolds eq. (3) has been discretized using the finite difference method. Thereafter, coupled solution of algebraic equations has been achieved by using Gauss-Seidel iterative technique. Numerical results reported in this paper have been generated using 51(N_θ) x 21(N_z) grids. This grid size has been arrived based on the grid independence test. The numerical solution is carried out as per the following steps:

1. For prescribed values of G, δ, ε, α and for an assumed value of the attitude angle ϕ, the fraction film content φ is computed by solving eq. (3). Convergence is attained when $\sum_{i=1}^{m}\sum_{j=1}^{n}\left|\left(\varphi_{i,j}\right)^{N+1} - \left(\varphi_{i,j}\right)^{N}\right| \Big/ \sum_{i=1}^{m}\sum_{j=1}^{n}\left|\left(\varphi_{i,j}\right)^{N+1}\right| \le 10^{-5}$.
2. Bearing force components $\bar{F}_x$ and $\bar{F}_y$ are calculated and if $\left|\bar{F}_y / \bar{F}_x\right| > 10^{-4}$, then another value of ϕ is assumed until the convergence.
3. A finite perturbation of displacements $(\Delta X = \Delta Y = 0.001C_r)$ and velocities $(\Delta\dot{X} = \Delta\dot{Y} = 0.001C_r\omega)$ are given to the journal centre and bearing forces are calculated to obtain the stiffness and damping coefficients.
4. Steps 1-3 are repeated for various input parameters.

4. Results and discussion

This section presents the numerical results pertaining to the performance parameters of elliptic bore journal bearing and stability of rigid rotor mounted on elliptic bore journal bearings. All the results reported in this paper have been generated for L/D =1. For developing the confidence in the proposed model, the dimensionless stiffness and damping coefficients numerically obtained using the present model have been compared with the work of ref.[17] in Figs. 2(a) and 2(b). Good correlations between the present numerical results (shown with lines) and work of ref.[17] (shown with different markers) can be seen in these figures. Thus, the overall correctness of the results achieved from the proposed model has been established.

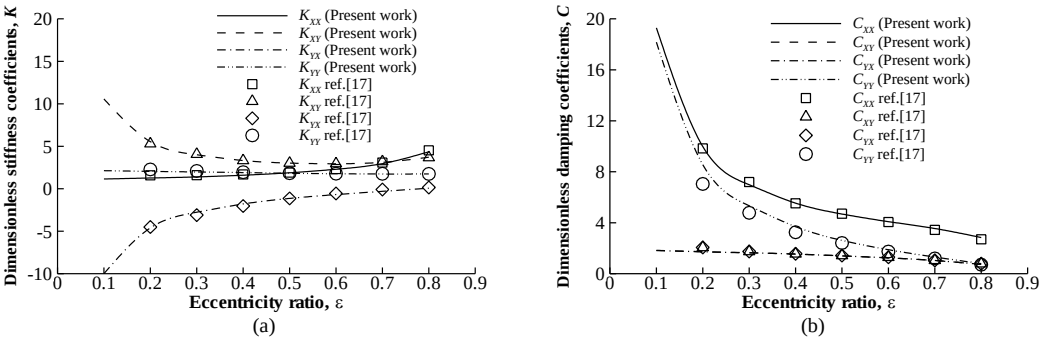

Fig. 2. Comparison of stiffness and damping coefficients with findings of ref. [17] (G = 0 and α = 0.1)

Figures 3(a) and 3(b) demonstrate the pressure profiles at the mid-plane of bearing for different values of the bore orientations (δ = 0°, 30°, 60°, 90°, 120°, and 150°). Large magnitude of pressure profiles are seen in these figures with the circular bore (i.e. G = 0). It is obvious from these figures that the pressure developed inside the circular bore bearing is larger as compared to elliptic bore bearing irrespective of the orientation of the elliptic bore. However, the orientation of elliptic bore has significant influence upon the magnitude and profile of the pressure. It can be seen that pressure inside the elliptic bore is on the higher side for δ > 90°. This is due to the film shape i.e. a convergent zone is encountered first in the moving direction of lubricant for δ > 90°.

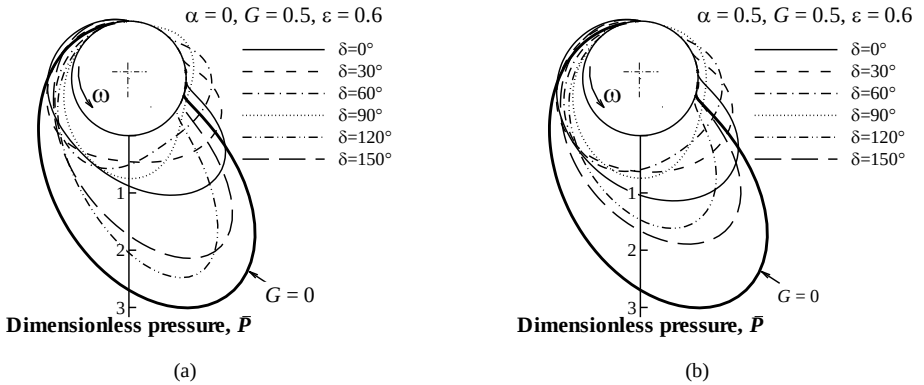

Fig. 3. Pressure profile in the lubricating films at bearing mid planes for two different input parameters

All the results for the performance parameters (excluding pressure profiles) reported in this paper have been expressed in relative form (i.e. ratio of the performance parameter with the elliptic bore bearing to the performance parameter with cylindrical bore bearing of radius equal to the minor radius of the elliptic bore bearing) for bringing the clarity in the comparisons. The results for load (W/W_0), coefficient of friction (f/f_0), and stability parameter (M_{cr}/M_{cr0}) have been presented in the Figs. 4-6 where the subscript '0' signifies the value of a parameter for the circular bore bearing. The results reported in these figures have been generated for combinations of operating parameters: α = 0 and 0.5, δ = 0°, 30°, 60°, 90°, 120°, and 150°; and G = 0.1, 0.2, 0.3, 0.4, and 0.5 in order to have generality in the comparisons.

The variation of load factor (W/W_0) with eccentricity ratio (ε) for combinations of values of α, δ, and G are shown in Figs. 4(a)-4(d). It can be seen in these figures that load carrying capacity reduces for elliptic bores compared to the circular bore and bore orientation has a profound influence on the load carrying capacity. Also the load carrying capacity decreases with increasing values of ellipticity parameter (G). Marginal increase in the load carrying capacity has been observed with few combinations of α, δ, and G, particularly at very low values of eccentricity ratio (ε). This happens due to the relatively large pressure generation region and magnitudes in elliptic bore bearing in comparison to circular bore bearing due to the formation of physical wedge.

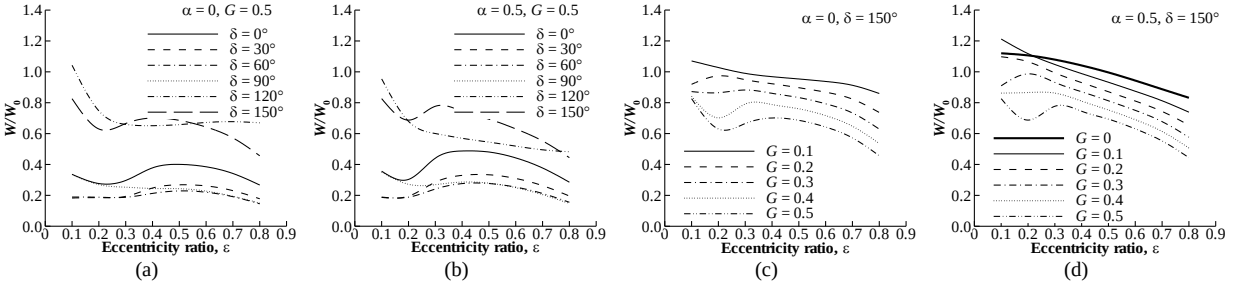

Fig. 4. Variation of W/W_0 with eccentricity ratio

Figures 5(a)-5(d) show the variation of friction parameter (f/f_0) with eccentricity ratio (ε) for combinations of δ and G. It can be seen from these figures that the orientation of the elliptic bore influences the friction parameter for both Newtonian and non-Newtonian lubricants. Comparing Figs. 5(c) and 5(d), it is observed that the ellipticity parameter (G) does not have vital effect on the friction parameter. However, it can be concluded in general that ellipticity of the bore increases the coefficient of friction in comparison with a circular bore.

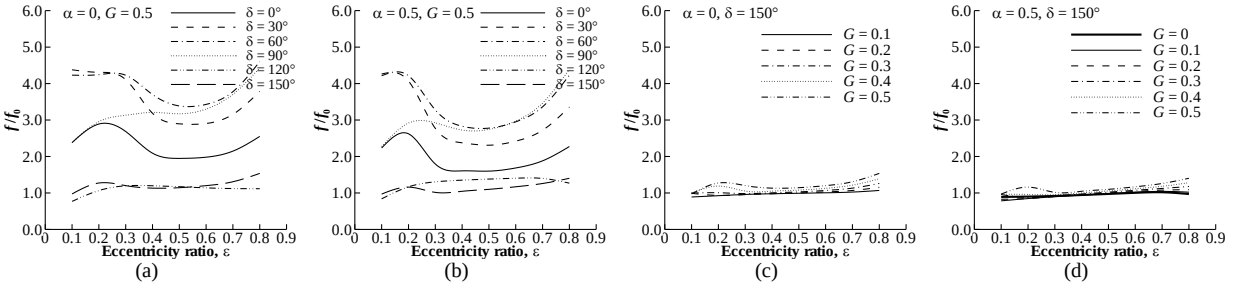

Fig. 5. Variation of f/f_0 with eccentricity ratio

Figures 6(a)-6(d) illustrate the variation of the stability parameter (M_{cr}/M_{cr0}) with eccentricity ratio (ε) for the combinations of input parameters: α, δ, and G. It can be seen that for Newtonian lubricant $\alpha = 0$, the stability parameter (M_{cr}/M_{cr0}) is greater than 1 at high values of G, ε and $\delta \geq 90°$. This implies that elliptic bore bearing provides higher stability limit in comparison to circular bore. It can be stated that in general the ellipticity of the bearing bore is helpful in improving the stability of the rotor. On the other hand for non-Newtonian fluids (refer Figs. 6(b) and 6(d)), it is seen that the stability parameter is generally less than 1 for $0.3 \leq \varepsilon \leq 0.6$. The stability with non-Newtonian fluid is better with elliptic bore if bearings are heavily loaded. Higher stability with elliptic bore bearing compared to circular bore is due to the fact that the former generally has higher dissipation of whirl energy resulting in increment of stability limit speed.

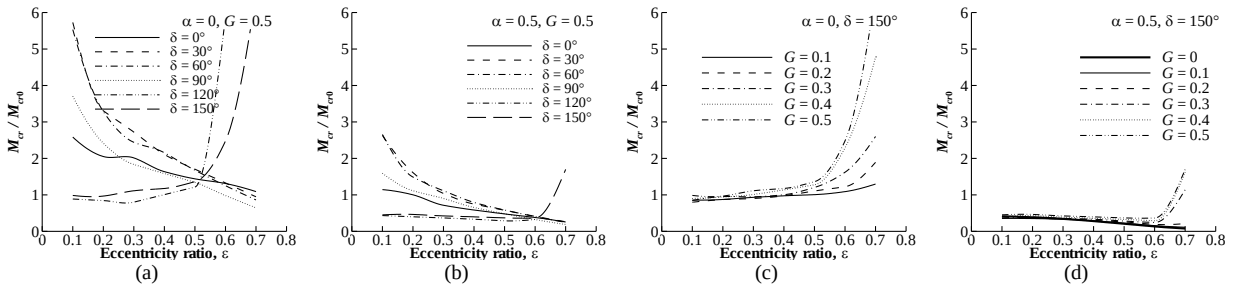

Fig. 6. Variations of M_{cr}/M_{cr0} with eccentricity ratios

5. Concluding remarks

The performance of hydrodynamic journal bearing incorporating the effects of ellipticity of the bore and non-Newtonian rheology of lubricant has been investigated in this paper. The bearing coefficients (stiffness and damping) have been computed using the finite perturbation approach for exploring the linear stability of a rigid rotor. Moreover based on the investigations reported herein, the following conclusions have been drawn:

- Elliptic bore which gets generated due to the operational issues of bearing is not helpful for improving the load carrying capacity and reducing the friction coefficient.
- Elliptic bore bearing in general enhances the stability of the rotor-bearing system for any orientation of elliptic bore.
- Shear thinning of lubricant in general decreases the load carrying capacity of elliptic bore bearing, but an increase in load carrying capacity is achieved for $G < 0.2$ and $\varepsilon < 0.3$.
- Shear thinning of lubricant in general results in decrease of stability of the rotor-bearing system.

References

[1] Berthe D, Fantino B, Frêne J, Godet M. Influence of shape defects and surface roughness on the hydrodynamics of lubricated systems. J Mech Eng Sci 1974;16:156–9.
[2] Crosby WA. An investigation of the performance of a journal bearing with a slightly irregular bore. Tribol Int 1992;25:199–204.
[3] Mishra PC, Pandey RK, Athre K. Temperature profile of an elliptic bore journal bearing. Tribol Int 2007;40: 453-458.
[4] Goenka PK, Booker JK. Effect of surface ellipticity on dynamically loaded cylindrical bearings. J Tribol 1983;105:1–9.
[5] Bonneau O, Frêne J. Influence of bearing defects on dynamical behavior of an elastic shaft. Int J Rotating Mach 1996;2:281–7.
[6] Bouyer J, Fillon M, Pierre-Danos I. Influence of wear on the behavior of a two-lobe hydrodynamic journal bearing subjected to numerous startups and stops. J Tribol 2007;129:205–8.
[7] Lund JW. Review of the concept of dynamic coefficients for fluid film journal bearings. J Tribol 1987;109:37–41..
[8] Choy FK, Braun MJ, Hu Y. Nonlinear effects in a plain journal bearing : part 1 — analytical study. J Tribol 1991;113:555–61.
[9] Flack RD, Kostrzewsky GJ, Barrett LE. Experimental and predicted rigid rotor stability threshold of axial groove and three-lobe bearings. Int J Rotating Mach 2002;8:27–33.
[10] Qiao G, Wang L, Zheng T. Linear stability analysis of a tilting-pad journal bearing system. J Tribol 2007;129:348–53.
[11] Chen SK, Chou HC, Kang Y. Stability analysis of hydrodynamic bearing with herringbone grooved sleeve. Tribol Int 2012;55:15–28.
[12] Weng CI, Chen CR. Linear stability of short journal bearings with consideration of flow rheology and surface roughness. Tribol Int 2001;34:507–16.
[13] Ene NM, Dimofte F, Keith Jr. TG. A stability analysis for a hydrodynamic three-wave journal bearing. Tribol Int 2008;41:434–42.
[14] Gautam SS, Meena L, Ghosh MK. Dynamic characteristics and stability of short wave journal bearings. Tribol Online 2010;5:92–5.
[15] Nicoletti R. Optimization of journal bearing profile for higher dynamic stability limits. J Tribol 2013;135:117021–1170213.
[16] Wada S, Hayashi H. Hydrodynamic lubrication of journal bearings. Bull JSME 1971;14:279–86.
[17] Swamy STN, Prabhu BS, Rao BVA. Stiffness and damping characteristics of finite width journal bearings with a non-Newtonian film and their application to instability prediction. Wear 1975;32:379–90.
[18] Elrod HG. A cavitation algorithm. J Tribol 1981;103:350–4.
[19] Kango S, Sharma RK, Pandey RK. Comparative analysis of textured and grooved hydrodynamic journal bearing. Proc Inst Mech Eng Part J J Eng Tribol 2013;228:82–95.
[20] Kango S, Sharma RK, Pandey RK. Thermal analysis of microtextured journal bearing using non-Newtonian rheology of lubricant and JFO boundary conditions. Tribol Int 2014;69:19–29.
[21] Qiu ZL, Tieu AK. The effect of perturbation amplitudes on eight force coefficients of journal bearings. Tribol Trans 1996;39:469–75.